View metadata, citation and similar papers at core.ac.uk

brought to you by CORE

provided by Elsevier - Publisher Connector

Journal of Advanced Research (2013) 4, 75–82

Cairo University

Journal of Advanced Research

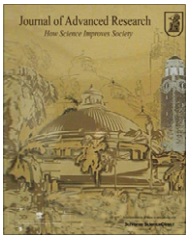

ORIGINAL ARTICLE

Synthesis and characterization of laminated Si/SiC composites

Salma M. Naga [a,*], Sayed H. Kenawy [a], Mohamed Awaad [a], Hamada S. Abd El-Wahab [a], Peter Greil [b], Magdi F. Abadir [c]

[a] *National Research Center, Ceramic Dept., Tahrir Str., Dokki, Cairo, Egypt*
[b] *Unversity of Erlangen-Nuernberg, Department of Materials Science (III), Erlangen, Germany*
[c] *Cairo University, Chemical Engineering Dept., Cairo, Egypt*

Received 16 November 2011; revised 20 January 2012; accepted 20 January 2012
Available online 24 February 2012

KEYWORDS

Laminates;
Si/SiC composites;
Microstructure;
Permeability;
Oxidation resistance

Abstract Laminated Si/SiC ceramics were synthesized from porous preforms of biogenous carbon impregnated with Si slurry at a temperature of 1500 °C for 2 h. Due to the capillarity infiltration with Si, both intrinsic micro- and macrostructure in the carbon preform were retained within the final ceramics. The SEM micrographs indicate that the final material exhibits a distinguished laminar structure with successive Si/SiC layers. The produced composites show weight gain of ≈5% after heat treatment in air at 1300 °C for 50 h. The produced bodies could be used as high temperature gas filters as indicated from the permeability results.

© 2012 Cairo University. Production and hosting by Elsevier B.V. All rights reserved.

Introduction

Porous SiC ceramics have drawn attention in the field of porous ceramics due to their superior properties, such as low thermal expansion coefficient, high thermal conductivity and excellent mechanical strength [1–3]. However, their brittleness limits their use in most structural applications. To improve fracture resistance in brittle material–matrix composites, the use of a weak interface that promotes crack deflection is necessary [4]. The earliest ceramics composites used as interfaces are boron nitride or carbon; however, these materials are prone to oxidation at high temperature. Porous-oxide layers seem to be an attractive alternative and have been successfully demonstrated as effective interface layers in laminated ceramic composites [5,6]. Laminated system consisting of porous-Al_2O_3 interfaces between Al_2O_3 bars showed markedly improved fracture resistance for these composites as compared with monolithic Al_2O_3 [5].

Clegg et al. [7] have produced laminated SiC with graphite interface layers. These multilayer SiC composites showed apparent toughness and fracture energy 5 and 200 times, respectively, higher than the typical values of monolithic – SiC. However, it was shown that laminated composites without weak interfaces also exhibited damage-tolerant behaviors [8,9].

* Corresponding author. Tel.: +20 233322445; fax: +20 233370931.
E-mail address: salmanaga@yahoo.com (S.M. Naga).

2090-1232 © 2012 Cairo University. Production and hosting by Elsevier B.V. All rights reserved.

Peer review under responsibility of Cairo University.
doi:10.1016/j.jare.2012.01.006

ELSEVIER Production and hosting by Elsevier

Due to its internal sintering, SiC ceramics are usually fabricated at extremely high temperature [10]. Thus the key problem is how to prepare porous SiC ceramics at relatively low temperature [11]. Usually, oxide with low sintering temperature may be added into the starting materials to form oxide bonded porous SiC ceramics [12]. The oxidation of SiC is well documented in the literature [13–15]. The oxidation can lead to the formation of SiO_2 and CO/CO_2 (passive oxidation), with an increase in weight and passivation of the surface, or to SiO and CO (active oxidation). In the latter case there is no passivating layer formed on the surface of the SiC and there is continual loss of material. Active oxidation however, is possible only at low oxygen partial pressure or very high temperature. In case of presence of water vapor the reactions are different, and an oxidation with continual removal of the oxidized layer is possible.

In the present study, a novel method of synthesizing laminated Si/SiC composite is described, by which SiC multilayer ceramic can be fabricated of biomorphic materials. The physical and mechanical properties of the samples will be investigated together with their oxidation resistance in air, microstructure and phase composition. The kinetics of oxidation is also studied.

Experimental

Specimen preparation

The substrates used in this study are flat woven-cellulosic fabric preforms, Fig. 1. It is a woven 100% cotton fabric with a plain structure 1/1 (usually called DUCK fabrics). It is heavy fabrics with high tensile strength (1.8 MPa) usually used in tents and fabric ceilings. It is a cotton woven plain fabric. The number of yarns/cm is 18 and the fabric weight (warp + weft) is 512 g/m^2. It possesses an air permeability of 4.68 (cm^3/cm^2/s) at 12.7 mm differential pressure (WG). The fabrics were cut to 10×10 cm^2 squares. About 15 plates were stacked together forming a plate with dimensions of $10 \times 10 \times 1$ cm^3. To obtain flat samples the cellulosic fabric layers are placed between two light weight ceramic plates applying a load of 10 N, so that they cannot deform during the carbonization process. A slow heating rate of 1 °C/min in N_2 atmosphere was applied up to 350 °C with a soaking time of 2 h at the peak temperature. On a second ramp the samples were heated at 1 °C/min up to 800 °C and kept at that temperature for 1 h, before cooling down to room temperature. The obtained carbon templates were used as preforms for the following infiltration process. Si powder (Elken HQ with particle size from 1 to 10 μm) dispersed in isopropyl alcohol in the presence of a dispersing agent (Hypermer; polyalkylene amine derivative) was used as infiltrant. The pyrolyzed carbon specimens were impregnated with two silicon slurries differing in silicon loading (4.5 wt.% and 8 wt.%), under a low pressure of 10^4 Pa for 1 h to ensure complete impregnation. After drying at 90 °C, heat treatment at 1500 °C with a soaking time of 2 h at the peak temperature in a graphite reactor under vacuum of ≈1 Pa resulted in the formation of a laminated porous Si/SiC composite. The obtained Si/SiC plates were cut into bars of $5 \times 1 \times 1$ cm^3 for further investigation.

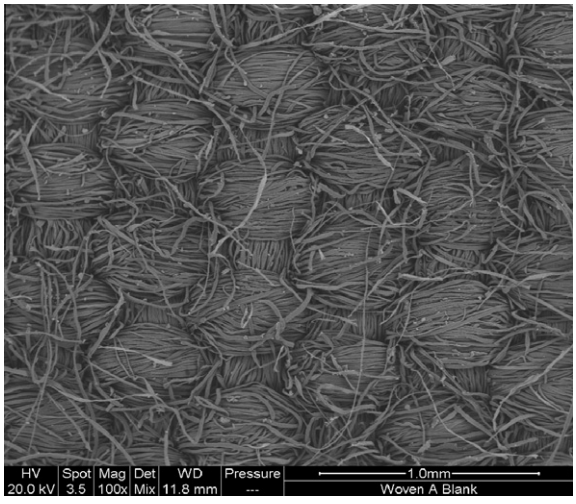

Fig. 1 Micrograph of textile fabric used to manufacture the ceramics.

Characterization

The bulk density and open porosity of the fabricated composites were evaluated using the Archimedes method (ASTM C-20) with water as liquid medium. X-ray diffraction analysis (XRD) of powdered samples using monochromatic Cu Kα radiation (D 500, Siemens, Mannheim, Germany) was used to identify crystalline reaction products. Microstructures were observed using scanning electron microscope (SEM) (Model XL 30, Philips, Eindhoven, Netherlands). Bending strength was measured using a three point bending test on a universal testing machine (Model 4204, Instron Corp., Danvers, Mass) at a crosshead speed of 1 mm/min. At least 10 specimens with the dimensions of $50 \times 10 \times 10$ mm were measured. The samples fracture toughness was determined on a single-edged notch specimen using the three-point bending method according to the procedure outlined in ASTM E399-90 (1992). The notch was made with a diamond saw. The samples were statically compression loaded until fracture at a cross head speed of 0.5 mm/min. The load–deflection curves were recorded continuously with a computer controlled testing machine (Model LRX-plus; L. Lloyd Instruments Ltd., Fareham, UK). The permeability of air through specimens was measured at 0.1 MPa of gas pressures difference in a permeation test cell. Permeability was determined according to Darcy's law.

$$K = \frac{qL\eta}{\Delta pA}$$

where q is the mass flow (m^3/s), L the sample thickness (m), η the air dynamic viscosity (Pa s), Δp the back pressure (Pa) and A is the sample area (m^2).

$$1 \text{ Darcy (D)} = 0.9869233 \times 10^{-12} \text{ m}^2, \quad \text{SI-unit of } K$$
$$= 1.02325 \times 10^{12} \text{ D}.$$

Mercury porosimetry (Model pore sizer 9320, Micromerities, USA) was used to measure the samples average pore size and pore area.

The thermal oxidation resistance of the Si/SiC composite was examined in air under static conditions at 1300 °C. The samples were kept at the peak temperature for definite time intervals. Then the samples were taken out, cooled in dissector

and weighted with accuracy ±0.1 mg. The total time of testing was 50 h.

Results and discussion

Carbonization

The pyrolysis of the cellulosic fabrics has a great effect on the properties of the composite. It is important to choose a pyrolysis temperature appropriate for avoiding distortion and crack formation during the carbonization. Fig. 2 shows the thermal gravimetric analysis (TG) curve of the raw textile. It shows that the weight loss started below 100 °C and was almost terminated at 500 °C. The maximum decomposition rate was in the temperature range of 245–400 °C. Mechanisms involved in the conversion of cellulose to carbon are [16]: (1) desorption of adsorbed water up to 150 °C, (2) splitting off of cellulose structure water between 150 °C and 240 °C, (3) chain scissions, or depolymerization, and breaking of C–O and C–C bonds within ring units evolving water, CO and CO_2 between 240 °C and 400 °C, (4) aromatization forming carbon layers above 400 °C and (5) completion of the decompositions and rearrangements, leaving a carbon template structure. Cellulose breaks down with a stepwise manner at 245–475 °C, and the total weight loss of about 75% (Fig. 2) occurred due to evolution of H_2O, CO_2 and volatile hydrocarbons from fragmentation reactions of the polyaromatic components. The mass loss of the textile preforms after carbonization up to 1000 °C is about 80 wt.%.

Microstructure

XRD patterns of the bodies sintered at 1500 °C Fig. 3a and b shows that the only phases present are β-SiC and Si. In both compositions, there is no evidence for residual carbon or crystalline SiO_2 phase. Fig. 3a shows an increase in the Si peak intensity due to the increase in the Si content (8%). The residual content of free silicon amounts to 11.8 vol.% in the specimen infiltrated with the 4.5 wt.% Si slurry and 30.8 vol.% for 8 wt.% Si slurry, respectively. The reaction mechanism of Si slurry with the porous carbon template can be divided into four stages [17]:

1. *Nucleation stage:* heterogeneous nucleation of nano-scaled SiC grains on the inner surface of the carbon template by reaction with Si vapor below the melting point of Si ($T < 1410$ °C).
2. *Initial stage:* Simultaneous nucleation of nano-grained and coarse-grained β-SiC after Si melt infiltration.
3. *Intermediate stage:* diffusion-controlled growth of the β-SiC layer into the carbon struts.
4. *Final stage:* dissolution of the nano-grained SiC in the Si melt and re-crystallization on coarse-SiC grains resulting in a coarsening of the coarse-grained SiC phase ($T > 1400$ °C).

The density of Si/SiC composites containing 4.5 wt.% Si and fired at 1500 °C is 0.7 g/cm^3 and their apparent porosity is 48.13%. Increasing Si content to 8 wt.% filled the body pre-existing pores with Si, increases the composite bulk density to 2.10 g/cm^3 and decreases the apparent porosity to 17.93%. Table 1 shows the densification parameters of the produced bodies.

A low temperature pyrolysis at 800 °C of the cellulosic fabrics followed by infiltration of Si into the skeletal carbonaceous preforms under pressure and firing at 1500 °C produces Si/SiC composites with structure of the native cellulosic fabrics, Fig. 4a. The gaps between carbon layers after carbonization were filled with silicon and exhibited a distinguished laminated microstructure, Fig. 4b. Fig. 4c indicates the development of a mixture of fine grain and needle-like SiC whiskers between the composite fibers. The needle-like whiskers had been grown in situ. They were grown by the vapor phase reaction between SiO and CO during the reaction [18]. The in situ grown SiC whiskers were observed by many authors during the synthesis of biomorphic SiC ceramics from mineralized cellulosic preforms [19–21].

Permeability measurement

The fluid permeability is an important parameter for porous ceramics. Liu et al. [22] indicated in their study that the gas permeability of the ceramics specimens is dependent on the average pore size than the open porosity. Plot of the gas flow rate vs. applied pressure gradient of Si/SiC composite

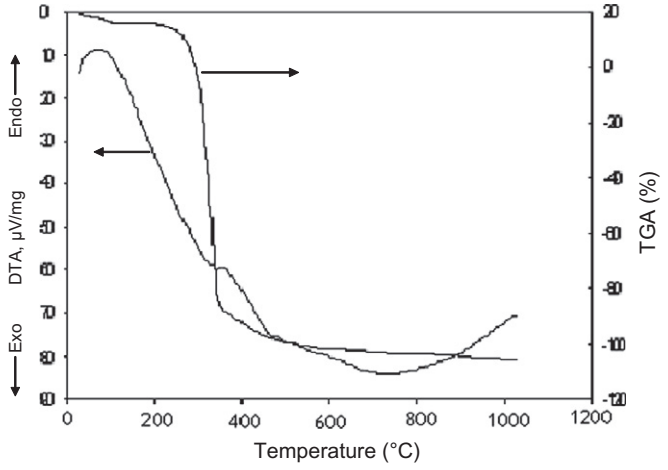

Fig. 2 DTA and TG curves of the raw textile.

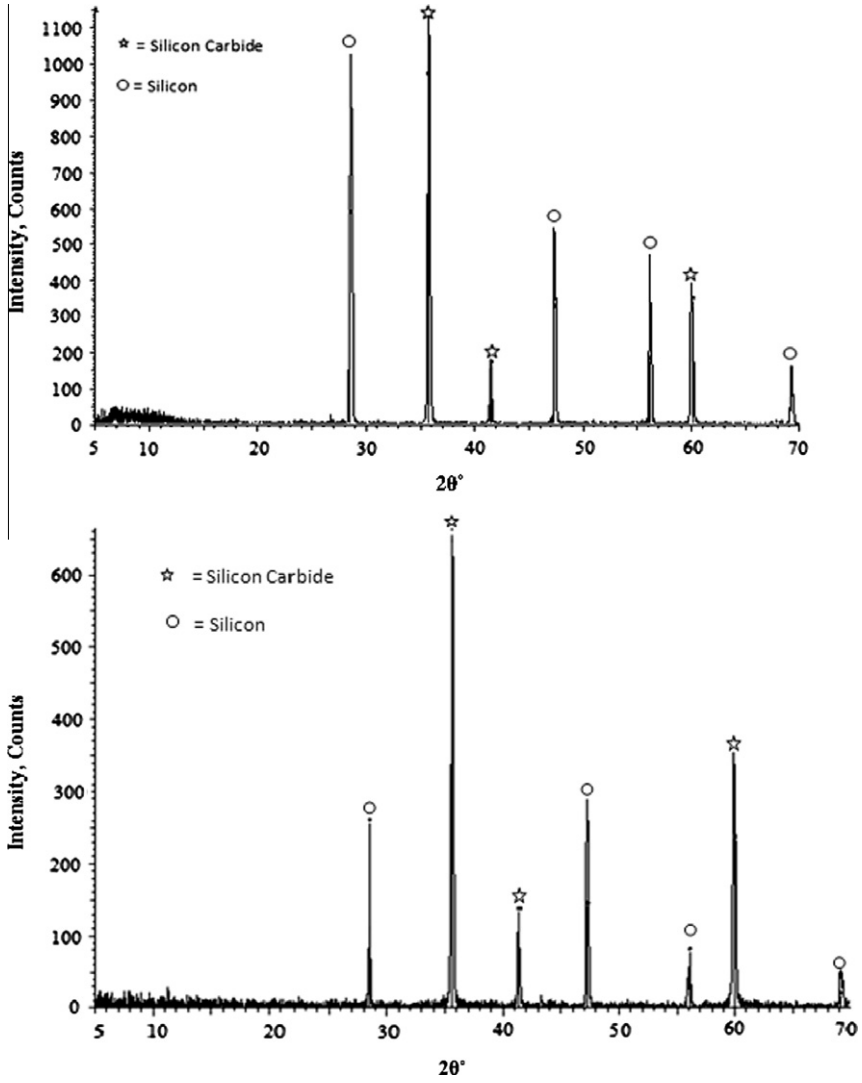

Fig. 3 XRD patterns of the bodies fired at 1500 °C. (a) Bodies containing 8 wt.% Si. (b) Bodies containing 4.5 wt.% Si.

Table 1 Pore size, pore distribution, apparent porosity and pore diameter of the laminated Si–SiC composite.

Sample	Pore diameter (μm)	Average pore diameter (μm)	Total pore area (m^2/g)	Porosity (%)	Pore diameter (μm)
Carbon substrate	65.63	0.162	57.91	79.55	0.0092
Si/SiC composites (4.5 wt.% Si)	16.75	0.106	17.19	59.23	0.0084

containing 4.5 wt.% Si is given in Fig. 5. This plot is linear, showing that the flow is in a good agreement with Darcy's law. Multiplying the slope of this line with the viscosity η of the fluid yields the permeability K. K results are illustrated in Table 1. In porous SiC ceramics, there are mainly two kinds of pores. Small pores derived from the stack of SiC particles, and large pores formed by burning out carbon particles [23]. More carbon content in the green bodies increases the number of the large pores, resulting in higher open porosity. The high porosity improves the connectivity of open pores and then reduces the tortuosity of pore channels. Furthermore, plenty of large pores formed as a result of burning out carbon particles enlarge the average pore diameter in porous SiC ceramics. The higher open porosity, large average pore diameter and lower tortuosity lead to the large Darcian permeability [24]. Due to the abrupt increase of the open porosity and pore size caused by the lamination of porous Si/SiC composite, more pore walls were formed, and the interaction between flowing gas and pore walls is enhanced. The Darcian permeability of the produced laminated Si/SiC composites was found to be 2.8×10^{-10} m^2, which is in the order of magnitude of gas filter supports, and, therefore, the produced bodies are suitable for several technological applications.

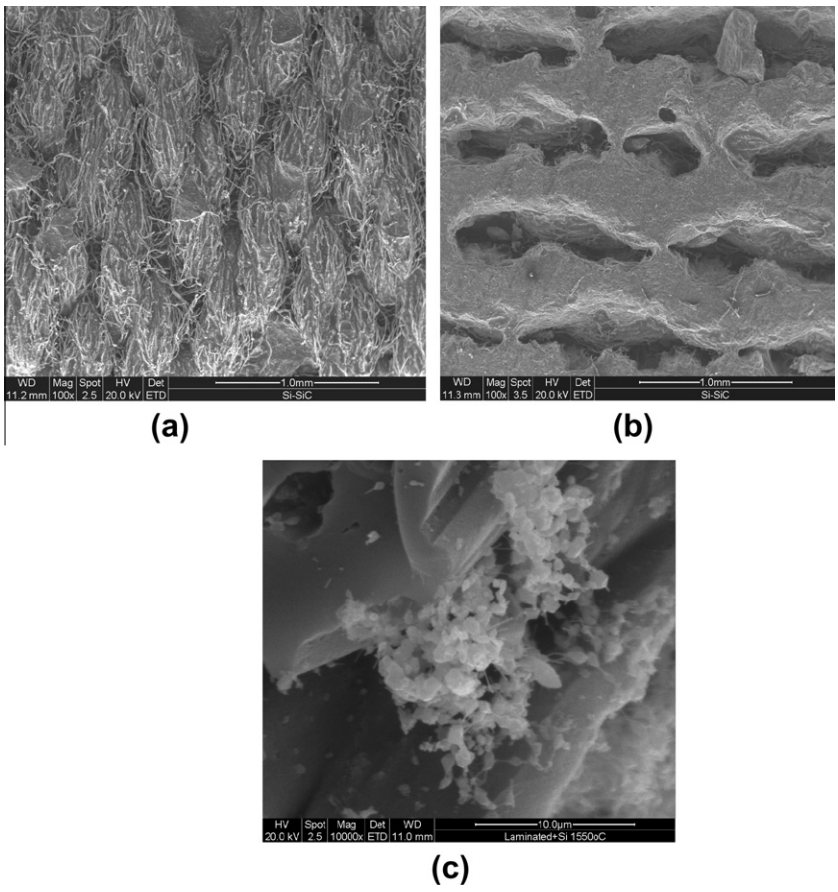

Fig. 4 SEM micrograph of laminated Si/SiC composite fired at 1500 °C. (a) Laminated Si/SiC composite single layer showing retention of the native fabric, architecture. (b) Cross section of laminated Si/SiC composite showing necks between the stacked layers. (c) Fine grains and whiskers of SiC.

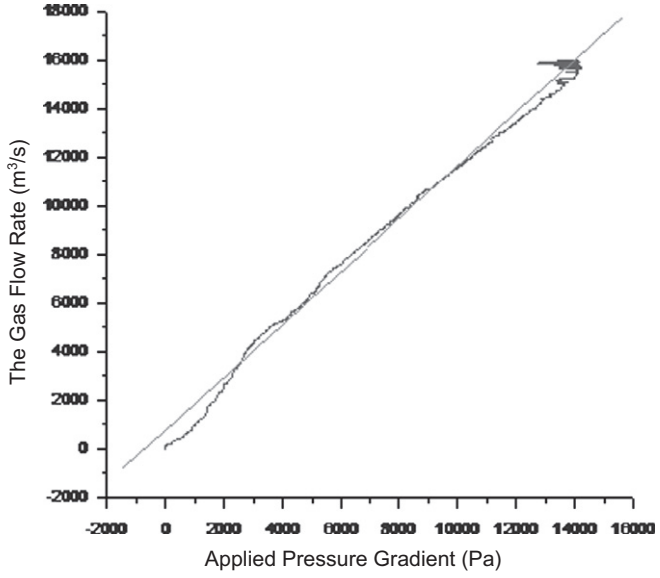

Fig. 5 The gas permeability of the Si/SiC composites containing 4.5 wt.% Si.

Pore analysis

The pore size distribution of the carbon substrate and the Si/SiC composite shows a variation in pore area, pore volume and size in the developed pore system of the composite. Table 1 shows that the size and distribution of pores greatly affected by the infiltration of carbon by Si, Fig. 6a and b shows the pore size distribution of the measured samples. Carbon

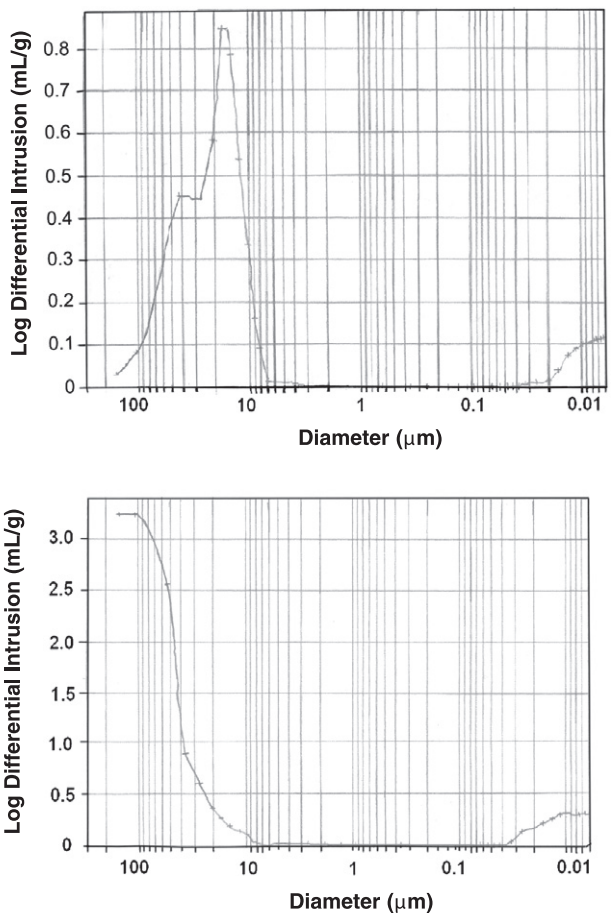

Fig. 6 The analysis of pore size distribution. (a) Carbon substrate pore size distribution. (b) Si/SiC composite pore size distribution.

substrate (Fig. 6a) shows pore proportion in the range of 150.99–31.26 μm, with some fine fraction concentrated in the range from 0.060 to 0.012 μm range. On the other hand, Si/SiC composites takes on a bimodal pore size distribution at 159.47 and 53.97 μm, with some in fine fraction 0.030–0.006 μm. Infiltration of C substrates decreases the open porosity. It seems that the acute viscous Si flow promotes the closure of small pores and the shrinkage of large pores, leading to the decrease in open porosity and pore size, Table 1.

Mechanical properties

Table 2 shows the bending strength of Si/SiC composite laminates. It is obvious that the bending strength of the composites infiltrated with 8 wt.% Si is higher than that infiltrated with 4.5 wt.% Si. The low porosity (17.93%) of the Si/SiC composites infiltrated with 8 wt.% Si played a significant role in increasing its bending strength. This suggested that the silicon content was the critical factor influencing the final bending strength. Accordingly, the mechanical properties of these materials can be considered as a continuous network of SiC with residual Si.

Si–SiC composites display a nonlinear stress–strain behavior when tensile loaded parallel to the fiber direction. This nonlinearity is related to the occurrence of damaging phenomena, mainly including multiple matrix microcracking and fiber matrix-debonding. They are often referred to as damageable elastic materials [27]. Fig. 7 shows that the crack deflection occurs at the Si/SiC–Si/SiC interface. Further loading causes the formation of some new cracks in the next Si/SiC layer. This process is repeated until all the Si/SiC layers are cracked, resulting in a saw-structure response.

Fracture toughness figures of bio-SiC; for crack propagation perpendicular to the axial direction; are in agreement with the results obtained in the present study [28]. The multilayer Si/SiC samples studied here sustain stress after the outset of fracture. The delamination phenomena allow for signification sample deformation before final breaking. The delamination mechanism, which provides a toughness effect, is responsible for the fracture toughness improvement. Crack cannot easily propagate from one layer to another, so that each layer fails singularly rather than sudden fracture. In the case of multilayers, two methods were used to enhance toughness, namely the introduction of weak interfaces or the presence of residual stresses. In the first case porous interlayers can be used; which is the situation in the present study. In such case, when a crack approaches a sufficiently weak interface, it deviates, moving along the interface itself; in this way the propagation of cracks from a layer to another is more difficult and the fracture energy increase. The residual silicon plays a role as well. It could divert the crack from the path of the minimum energy resulting in the fracture toughness increase.

Oxidation resistance

Fig. 8 shows the results of the heat treatment of SiC in air at 1300 °C for different time intervals. Increasing time of heat treatment from 2 h to 10 h gave rise for a slight weight gain increase from 1% to 1.6%. SiC oxidation in air starts above 900 °C [25] to give glassy silica layer according to the following equation:

$$SiC + 2O_2 \rightarrow SiO_2 + CO_2$$

The slight increase in the weight gain after heat treatment up to 10 h is due to the presence of CO_2. The reaction between SiO_2 and SiC causes the formation of volatile SiO and CO. The above secondary solid state reaction depends upon the O_2 activity in the interface and occurs at low CO_2 pressure, i.e.

Table 2 The permeability and physico-mechanical properties of Si/SiC.

Si content (wt.%)	Physical properties		Bending strength (MPa)	Permeability, K (D) (%)	Fracture toughness (MPa $m^{1/2}$)
	Bulk density (g/cm^3)	Apparent porosity (%)			
4.5	0.7	48.13	34	9.72E+00	2.66
8	2.1	17.93	42	–	–

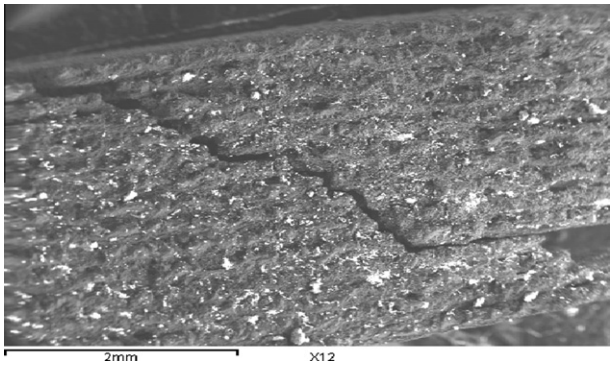

Fig. 7 Crack deflection occurs at the Si/SiC–Si/SiC interface.

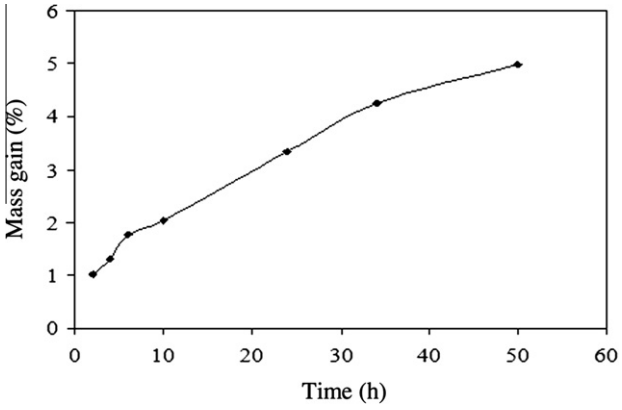

Fig. 8 Relation between weight gain and oxidation time.

at lower temperatures or short heat treatment intervals [26]. It seems that the rapid increase in the weight gain on increasing the heat treatment over 10 h is due to the easier transport of the volatile species.

Fig. 9 shows the microstructure of Si/SiC composite bodies heat treated at 1300 °C for 2 h. It shows a destroyed SiC fiber and SiO_2 grains, which confirmed the occurrence of the secondary solid state reaction and the formation of the volatile SiO and CO.

The kinetics of the oxidation reaction was studied using isothermal oxidation data. Because of the nature of the fibrous nature of the composite, the most likely controlling mechanism would be that of a diffusion controlled reaction. The relation between time of oxidation (t) and extent of reaction (X) for cylindrical shapes (typical of fibers) takes the form [29]:

$$t = k[X + (1 - X)\ln(1 - X)]$$

The plot of the RHS of the above equation against time is shown in Fig. 10. The linear character of the curve obtained (with a determination coefficient $R^2 = 0.995$) clearly supports the assumption that oxidation is controlled by diffusion of gaseous oxidation products through the silica layer.

Conclusions

1. Laminated Si/SiC composites derived from cellulosic fabrics were fabricated by process of lamination, carbonization, and infiltration with silicon slurry. The process is simple, low-cost and provides excellent shape-making capability.

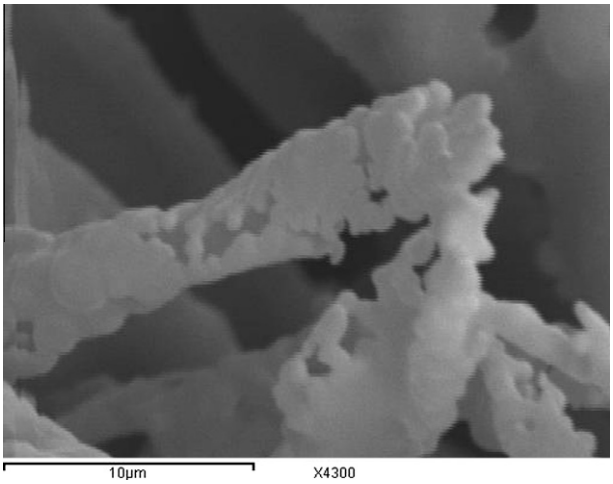

Fig. 9 SEM micrograph of laminated Si/SiC composite fired at 1500 °C after oxidation in air at 1350 °C for 2 h.

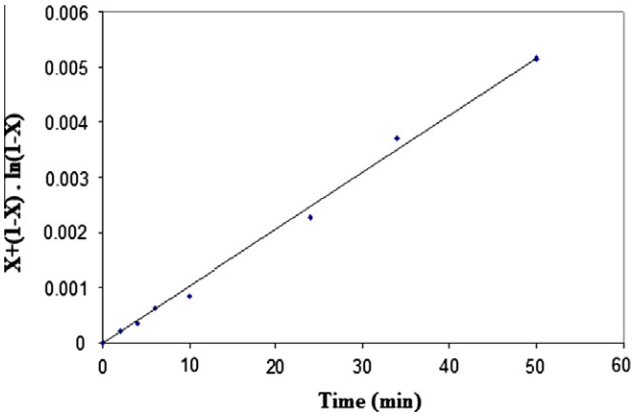

Fig. 10 Plot of $f(X)$ against oxidation time for diffusion controlled reaction.

2. The produced bodies exhibit a distinguished laminar structure with successive Si/SiC layers.
3. The biomorphous Si/SiC composites retained the features of the original native-cellulose fabrics. The produced porous materials possess a novel, directed pore morphology which cannot be reached conventional ceramic processing technologies.
4. The Si content of the composites has a significant effect on the mechanical properties.
5. The Darcian permeability of the produced composites is 2.8×10^{-10} m^2 which is the order of magnitude of gas filter supports and, therefore, may be suitable for several technological applications.
6. The oxidation reaction was found to be controlled by diffusion of gaseous products through the oxidation product layer.

References

[1] Rojas PC, Piderit GJ, Toro P. Development of open-pore silicon carbide foams. Key Eng Mater 1997;132–136:1731–4.

[2] Greil P. Advanced engineering ceramics. Adv Mater 2002;14:709–16.
[3] Passalacqua E, Freni S, Barone F. Alkali resistance of tap-cast SiC porous ceramic membranes. Mater Lett 1998;34: 257–62.
[4] Evans AG, Marshall DB. The mechanical behaviour of ceramic matrix composites. Acta Metal Mater 1989;37(10):2567–83.
[5] O'Brien MJ, Capaldi FM, Sheldon BW. A layered alumina composite tasted at high temperature in air. J Am Ceram Soc 2000;83(12):3033–40.
[6] Blanks KS, Kristoffersson A, Carlström E, Clegg WJ. Crack deflection in ceramic laminates using porous interlayers. J Eur Ceram Soc 1998;18(13):1945–51.
[7] Clegg WJ, Kendall KK, Alford NM, Button TW, Birchall JD. A simple way to make tough ceramics. Nature (London) 1990;347:455–7.
[8] Ebillat FR, Lamon J, Naslain R. Properties of multilayered interphase in SiC/SiC chemical–vapor infiltrated composite with "weak" and "strong" interfaces. J Am Ceram Soc 1998;81(9):2315–26.
[9] Kuo D-H, Kriven WM. Fracture of multilayer oxide composites. Mater Sci Eng A 1998;241(1–2):241–50.
[10] Omori M, Takei H. Pressureless sintering of SiC. J Am Ceram Soc 1982;65:C-92.
[11] Ding S, Zeng Y-P, Jiang D. In-situ reaction bonding of porous SiC ceramics. Mater Charact 2008;59:140–3.
[12] She J, Deng Z, Doni JD, Ohji T. Oxidation bonding of porous silicon carbide ceramics. J Mater Sci 2002;37:3615–22.
[13] Nickel KG. The role of condensed silicon monoxide in the active – to passive oxidation transition of silicon carbide. J Eur Ceram Soc 1992;9:3–8.
[14] Badini C, Fino P, Ortona A, Amelio C. High temperature oxidation of multilayered SiC processed by tape casting and sintering. J Eur Ceram Soc 2002;22:2071–9.
[15] Eaton HE, Linsey GD. Accelerated oxidation of SiC CMC's by water vapor and protection via environmental barrier coating approach. J Eur Ceram Soc 2002;22:2741–7.
[16] Griel P. Biomorphous ceramics from ligno-cellulosics. J Eur Ceram Soc 2001;21:105–18.
[17] Zollfrank C, Sieber H. Microstructure evolution and reaction mechanism of biomorphous Si SiC ceramics. J Am Ceram Soc 2005;88(1):51–8.
[18] Choi HJ, Lee JG. Continuous synthesis of silicon carbide whiskers. J Mater Sci 1995;30:1982–6.
[19] Shin Y, Wang C, Exarhos GJ. Synthesis of SiC ceramics by the carbothermal reduction of mineralized wood with silica. Adv Mater 2005;17(1):73–6.
[20] Hata T, Castro V, Fujiswa M, Imamura Y, Bonnamy S, Bronsveld P, et al.. Formation of silicon carbide nanorods from wood-based carbons. Fuller Nanotub Carbon Nanostruct 2005;13:107–13.
[21] Vyshnyakava K, Yushin G, Peressllentseva L, Gogotsi Y. Formation of porous SiC ceramics by pyrolysis of wood impregnated with silica. Int J Appl Ceram Technol 2006;3(6):485–90.
[22] Liu YF, Lui XQ, Weiand H, Meng GY. Porous mullite ceramics from national clay produced by gel casting. Ceram Int 2001;27:1–7.
[23] Ding S, Zhu S, Zeng Y, Jiang D. Fabrication of mullite-bonded porous silicon carbide ceramics by *in situ* reaction bonding. J Eur Ceram Soc 2007;27:2095–102.
[24] Ding S, Zeng Y, Jiang D. Gas permeability behavior of mullite-bonded porous silicon carbide ceramics. J Mater Sci 2007;42:7171–5.
[25] Guo Q, Song J, Liu L, Zhang B. Relationship between oxidation resistance and structure of B_4C/SiC/C composites with self-healing properties. Carbon 1999;37:33–40.
[26] Fitzer E, Ebi R. Kinetic studies on the oxidation of silicon carbide. In: Proceedings of the third international conference on silicon carbide held at Miami Beach, Florida; 1973.
[27] Naslain RN. SiC–matrix composites: nonbrittle ceramic for thermo-structural application. Int J Appl Ceram Technol 2005;2(2):75–84.
[28] Presas M, Pastar JY, Segurado J, Gonjàlez C. Strength and toughness of cellular SiC at elevated temperature. Eng Fail Anal 2009;16:2598–603.
[29] Orfao JJM, Matins FG. Kinetic analysis of thermogravimetric data obtained under linear temperature programming. Therm Chim Acta 2002;390:195–211.